



ER stress-associated CTRC mutants decrease stimulated pancreatic zymogen secretion through SIRT2-mediated microtubule dysregulation



Marcelo G. Binker^a, Daniel Richards^a, Herbert Y. Gaisano^b, Laura I. Cosen-Binker^{a, b, *}

^a CBRHC Research Center, Buenos Aires, Argentina

^b Departments of Medicine and Physiology, University of Toronto, Toronto, Ontario, Canada

ARTICLE INFO

Article history:

Received 23 April 2015

Accepted 15 May 2015

Available online 28 May 2015

Keywords:

CTRC

ER stress

Pancreatic zymogen secretion

SIRT2

Microtubule dysregulation

ABSTRACT

Pancreatitis has been suspected for a long time to have an autodigestive genesis. The main events occurring in the pancreatic acinar cell that initiate acute pancreatitis include inhibition of zymogen secretion and intracellular activation of proteases. Chymotrypsin C (CTRC) is a protective protease that limits trypsin and trypsinogen proteolytic activity. Hereditary pancreatitis-associated CTRC mutants such as p.A73T and p.G61R precipitate within the endoplasmic reticulum (ER) causing ER stress. We found that expression of these mutants reduces amylase secretion from carbachol-stimulated rat pancreatic acinar cells AR42J and isolated mice pancreatic acini. Furthermore, this expression also reduces the levels of acetylated tubulin by increasing both the levels and phosphorylation of the deacetylase SIRT2. Remarkably, inhibition of SIRT2 not only greatly recovers tubulin acetylation, but also amylase secretion in pancreatic acinar cells and isolated acini. However, SIRT2 inhibition does not rescue secretion of the CTRC mutants. These results strongly suggest that CTRC variants associated to ER stress inhibit secretagogue-stimulated pancreatic zymogen secretion by altering microtubule stability. Of note, the extent of this inhibition correlates with the degree of ER stress exhibited by the particular CTRC variant.

© 2015 Elsevier Inc. All rights reserved.

1. Introduction

Pancreatitis is an inflammation of the pancreas that has been suspected for more than a century to have an autodigestive genesis [1]. The main events occurring in the pancreatic acinar cell that initiate acute pancreatitis include inhibition of zymogen secretion and intracellular activation of proteases [2]. In the well-established experimental model of supramaximal cerulein-induced acute pancreatitis, zymogens exhibit missorting and co-localization with lysosomal cathepsin B within large cytoplasmic vacuoles, where trypsinogen is cleaved and activated [3]. The premature activation of trypsinogen within the pancreatic cell triggers the activation cascade of all pancreatic digestive zymogens [4]. The etiologies linked to pancreatitis include gallstones, alcohol, trauma, infections, immune and genetic factors [5]. Hereditary pancreatitis involving mutations in pancreatic enzymes is

suspected when a recurrence of acute episodes occurs, particularly in young people [6].

Human chymotrypsin C (CTRC) is a digestive protease synthesized and secreted by the pancreatic acinar cell as a proenzyme, which is activated by trypsin in the duodenum. CTRC is responsible for the degradation of human trypsin and trypsinogen isoforms with high specificity, ensuring a protective mechanism that limits trypsin and trypsinogen proteolytic activity [7]. To the present date, at least 32 CTRC mutants have been investigated and those that correlate with a pathological setting are the ones considered to be risk factors for chronic pancreatitis [8]. No pathogenic gain-of-function for CTRC mutants have been described [8]. Only CTRC variants involving a loss-of-function have been associated to disease, which is suspected to be a consequence of a catalytic defect, a proteolytic instability, or a distorted secretion [8,9]. Within this last group, CTRC variants such as p.A73T that result in a misfolded protein, precipitate within the endoplasmic reticulum (ER) causing ER stress, which is characterized by an increased up-regulation of X-box-binding protein 1 (XBP1), binding immunoglobulin protein (BiP) and calreticulin mRNAs [8,10]. The extent of this ER stress correlates with the magnitude in the loss of CTRC secretion

* Corresponding author. CBRHC Research Center, Buenos Aires, 1425, Argentina.
E-mail address: licb@cbrhc.org (L.I. Cosen-Binker).

exhibited by acinar cells expressing these variants [8]. However, expression of CTRC mutants that present a catalytic defect or a proteolytic instability is not associated to ER stress [8].

The secretory granules of the exocrine pancreas, zymogen granules (ZG), are apically bound post-Golgi carrier vesicles that underlie the regulated exocytotic pathway [11]. While the docking and access of mature secretory vesicles to the plasma membrane for exocytic release are regulated by the actin cytoskeleton [12], the vectorial delivery of ZG to the apical cell surface requires an intact microtubule system which contains its microtubule organizing center, and consequently the microtubular minus ends, close to the apical membrane domain [11,13,14]. The microtubule-disrupting agent colchicine followed by cerulein stimulation (maximal and supramaximal) induces transport vesicles to accumulate in the supranuclear region, inhibiting pancreatic secretion [15]. In contrast, the microtubule stabilizer taxol not only decreases the inhibition of pancreatic secretion, but also diminishes serum amylase level, pancreatic edema, and histological alterations induced by cerulein hyperstimulation [15].

The purpose of this study is to investigate the secretagogue-stimulated secretion in pancreatic acinar cells and isolated acini expressing CTRC mutants associated to ER stress.

2. Materials and methods

2.1. Antibodies and reagents

Rabbit anti-SIRT2 antibody and AGK2 were from Santa Cruz Biotechnology (Dallas, TX). Rat anti-phospho-SIRT2 antibody was from ActiveMotif (Carisbad, CA). Rabbit anti-HDAC6 antibody was from Abcam (Cambridge, MA). Mouse anti- α -tubulin, mouse anti-acetylated-tubulin, and mouse anti-actin antibodies, carbamoylcholine chloride (Carbachol), bovine serum albumin (BSA) and dexamethasone were from Sigma Chemical Co (St. Louis, MO). Dulbecco's Modified Eagle Media (DMEM), DMEM/F-12, OptiMEM, penicillin/streptomycin solution, fetal bovine serum (FBS), protease inhibitor cocktail and halt phosphatase inhibitor cocktail were from LifeTechnologies (Grand island, NY).

2.2. Recombinant adenovirus

Adenovirus carrying human wild-type (WT) CTRC and mutants p.A73T and p.G61R were described previously [8,10]. CTRC constructs contained a GluGlu epitope tag at the C terminus.

2.3. Cell culture and viral infections

Rat pancreatic AR42J acinar cells (ATCC, Manassas, VA) were maintained in DMEM supplemented with 20% heat-inactivated FBS, 2 mM glutamine, 100 nM dexamethasone to induce differentiation [16], and 1% penicillin/streptomycin solution, at 37 °C in a 5% CO₂ humidified atmosphere. Prior to infection, AR42J cells were washed with D-MEM/F-12 medium, plated into 35 mm wells (10⁶ cells per well) and incubated for 1 h at 37 °C in a 5% CO₂ humidified atmosphere. Cells were infected with 2 × 10⁸ pfu/ml final adenovirus concentrations in 1 ml OptiMEM supplemented with 2 mM glutamine, 100 nM dexamethasone and 1% penicillin/streptomycin, and experiments were performed 24 h later.

2.4. Dispersed acini preparation and viral infections

Mice were treated according to the Federal Guidelines for Animal Care, and the Institutional Animal Care and Use Committee approved the animal research protocol.

The preparation of isolated pancreatic acini from mice was performed by a mechanical and enzymatic dissociation technique as previously described [17,18]. The acini were resuspended in oxygenated Krebs-Ringer-HEPES (KRH) buffer supplemented with minimal essential and non-essential amino acid solution and glutamine. Prior to infection, acini were washed with D-MEM/F-12 medium, plated into 35 mm wells (~10⁶ cells per well) and incubated for 1 h at 37 °C in a 5% CO₂ humidified atmosphere. Cells were infected with 2 × 10⁸ pfu/ml final adenovirus concentrations in 1 ml D-MEM/F-12 medium supplemented with 0.1% BSA, 1 mM sodium pyruvate and 1% penicillin/streptomycin solution, and experiments were performed 24 h later.

2.5. Amylase secretion

AR42J cells and acini were stimulated with 80 μ M carbachol for 1 h at 37 °C. Amylase released into the supernatant and amylase content of the cell pellet were determined by a colorimetric method. 'Total amylase' is defined as the summation of the amylase content in the respective cell pellet plus supernatant, and the amylase secreted into the supernatant is expressed as a percent of total amylase.

2.6. Cell lysate preparation

After equilibration (20 min, 37 °C), infected cells were subjected to the indicated stimulation, and then terminated by adding excess volume of ice-cold KRH buffer. AR42J cells or acini were then washed twice with phosphate buffered saline (PBS). Subsequently, 200 μ l reporter lysis buffer (Promega, Madison, WI), 4 μ l protease inhibitor cocktail and 2 μ l halt phosphatase inhibitor cocktail were added and the cells were pelleted by centrifugation (300 g, 4 °C). The protein concentration of the supernatant was measured with the Micro BCA Protein Assay Kit (Thermo Scientific, Waltham, MA).

2.7. Immunoblotting

Protein content of all samples was determined with the Micro BCA Protein Assay Kit. Samples of conditioned media or cell lysates supernatants were dissolved in Laemmli buffer and boiled for 5 min. Equal amounts of protein from conditioned media or cell lysates supernatants were loaded, separated by 8% SDS-PAGE and transferred to nitrocellulose membranes (Bio-Rad, Waltham, MA). Blots were blocked for 1 h in Tris-buffered saline/0.1% Tween-20 containing 5% BSA and then incubated overnight with the corresponding primary antibody (1:1000 dilution) in Tris-buffered saline/0.1% Tween-20 containing 0.5% BSA at 4 °C. After three washes with Tris-buffered saline/0.1% Tween-20, the respective antigen-antibody complexes were identified by appropriate peroxidase-conjugated secondary antibodies and enhanced chemiluminescence (Amersham, Arlington Heights, IL). To detect the Glu-Glu tag, a horseradish peroxidase (HRP)-conjugated goat polyclonal antibody (Abcam) was used at a dilution of 1:10000. Quantification was performed by densitometry using Scion Image software (National Institutes of Health). Levels for the analyzed proteins were expressed as fold-increase over the control conditions.

2.8. Immunoprecipitation

Lysates containing equal amounts of protein were clarified by centrifuging at 12,000 g for 10 min. Supernatants were precleared for 40 min using Protein G-Sepharose beads (Pharmacia Biotech, Buckinghamshire, UK) and then incubated with the corresponding

first antibody for 1 h. Immune complexes were captured using Protein G-Sepharose beads, which were washed four times with lysis buffer containing 1 mM Na_3VO_4 . Protein content of all samples was determined by Micro BCA Protein Assay Kit, and equal amounts of these samples were dissolved in Laemmli buffer, boiled for 5 min, separated on SDS-PAGE, and transferred to nitrocellulose membranes. Separated proteins and the respective antigen–antibody complexes were identified by appropriate peroxidase-conjugated secondary antibodies and enhanced chemiluminescence. Quantification was performed by densitometry using Scion Image software. Levels for the analyzed proteins were expressed as fold-increase over the control conditions.

2.9. Statistical analysis

Data correspond to at least three independent experiments, each of which was done in triplicate. Results are presented as mean \pm standard error (SE). Student's *t*-test was used to evaluate data. Significant differences were considered with values of $p < 0.05$.

3. Results

3.1. Reduced amylase secretion from Cch-stimulated pancreatic acinar cells and isolated acini expressing ER stress-associated CTRC mutants

We first investigated amylase secretion as a measure of zymogen enzyme content release. Rat pancreatic acinar cells AR42J and isolated mice pancreatic acini were infected with distinct CTRC adenoviruses and then stimulated with a maximal dose of the secretagogue carbachol (Cch, 80 μM , 1 h). In basal unstimulated conditions, no differences were detected in either amylase release

(Fig. 1A and B) or total amylase content (data not shown). While non infected-control cells and cells infected with either the empty vector (EV) or wild type (WT) CTRC did not exhibit significant differences in Cch-stimulated amylase release ($27.8 \pm 1.1\%$, $26.1 \pm 1.2\%$ and $26.2 \pm 1.2\%$ in AR42J cells and $32.3 \pm 1.4\%$, $30.2 \pm 1.6\%$ and $29.8 \pm 1.8\%$ in acini, respectively; Fig. 1A and B), CTRC mutants associated to ER stress, p.A73T and p.G61R [10,12], decreased Cch-stimulated amylase release to values of $18.5 \pm 1.1\%$ and $12.9 \pm 1.3\%$ in AR42J cells (representing a reduction of 33.5% and 53.6% compared to controls, respectively; Fig. 1A and B), and to $22.4 \pm 1.3\%$ and $16.7 \pm 1.1\%$ in acini (reduction of 30.7% and 48.3%, respectively; Fig. 1A and B). Of note, p.G61R CTRC, which induces a greater ER stress than p.A73T CTRC [8], is the variant that exhibited a stronger inhibition of amylase secretion. Meanwhile, expression of the micro-deletion CTRC variant p.K247_R254del (p.247-254 Δ), which is linked to a catalytic defect and proteolytic instability, but does not induce ER stress [10], did not present significant differences in Cch-stimulated amylase release ($25.6 \pm 1.1\%$ and $29.6 \pm 1.9\%$ in AR42J cells and acini, respectively; Fig. 1A and B).

3.2. Reduced acetylated tubulin levels in acinar cells and acini expressing ER stress-associated CTRC mutants

The delivery of ZG to the apical cell surface requires intact microtubules [11,13,14], which in acinar cells are more stable than in many other cell types [13]. As we suspected that CTRC mutants associated to ER stress could be altering microtubule stability, we then examined the protein levels of α -tubulin and acetylated tubulin. As observed in Fig. 1C and D, no differences in α -tubulin levels were detected neither in AR42J cells nor in acini, whether or not they were infected with the different CTRC adenoviruses. When we analyzed the expression of acetylated tubulin, non infected cells and cells infected with EV, WT CTRC or p.247-254 Δ CTRC exhibited

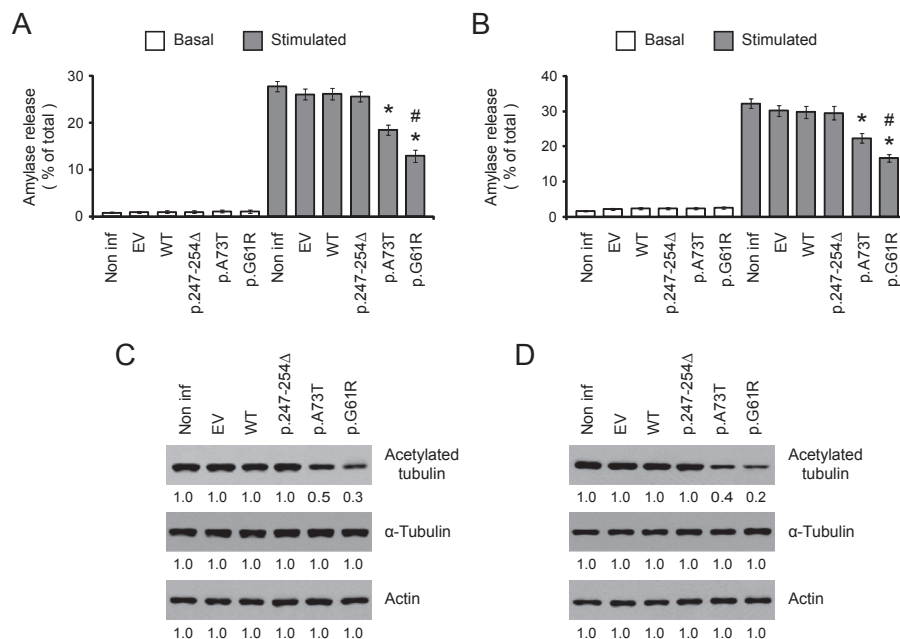


Fig. 1. Carbachol-stimulated acinar cells and acini expressing ER stress-associated CTRC mutants exhibit diminished amylase secretion and tubulin acetylation. Rat pancreatic acinar cells AR42J (A and C) and isolated mice pancreatic acini (B and D) were infected with the empty vector (EV), wild type (WT) CTRC, p.K247_R254del (p.247-254 Δ) CTRC, p.A73T CTRC or p.G61R CTRC, or were non infected (controls). (A–B) Infected and non infected cells and acini were incubated in KRH for 2 h and then stimulated with a maximal dose of the secretagogue carbachol (Cch, 80 μM , 1 h) or further incubated with KRH. Amylase secreted into the media was determined and expressed as a percentage of the total cellular amylase. * $p < 0.05$ and # $p < 0.05$ compared to Cch-stimulated non infected and p.A73T infected cells, respectively. (C–D) Levels of α -tubulin, acetylated tubulin, and actin (loading control) were analyzed in cell lysates of both infected and non infected cells. Representative immunoblots and densitometric analysis are shown.

the same levels (Fig. 1 C and D). However, both CTRC mutants p.A73T and even more significantly p.G61R, presented a notorious decrease in acetylated tubulin levels both in AR42J cells and acini (Fig. 1 C and D).

3.3. Elevated expression and phosphorylation of deacetylase SIRT2 in acinar cells and acini expressing ER stress-associated CTRC mutants

Microtubule deacetylation is performed by the classical class II histone deacetylase family member 6 (HDAC6) and the class III sirtuin deacetylase type 2 (SIRT2) [19]. Thus, we evaluated the levels of these deacetylases in our cell systems. Fig. 2A and B shows that no differences in HDAC6 levels were detected neither in AR42J cells nor in acini, whether or not they were infected with the different CTRC adenoviruses. Conversely, while non infected cells or cells infected with EV, WT CTRC or p.247-254Δ CTRC displayed the same levels of SIRT2, both CTRC mutants p.A73T and even more markedly p.G61R presented an increase in the levels of this protein in both AR42J cells and acini (Fig. 2A and B).

Subsequently, we assessed the phosphorylation status of immunoprecipitated SIRT2. While expression of WT CTRC did not cause SIRT2 phosphorylation, p.A73T and p.G61R CTRC led to a detectable phosphorylation of SIRT2 in both AR42J cells and acini (Fig. 2C and D). Of note, SIRT2 phosphorylation resulted more prominent in cells and acini infected with p.G61R CTRC (Fig. 2C and D).

3.4. Inhibition of SIRT2 greatly recovers tubulin acetylation levels in acinar cells and acini expressing ER stress-associated CTRC mutants

We next investigated the impact of SIRT2 inhibition on tubulin acetylation. The SIRT2 specific inhibitor AGK2 raised the acetylated tubulin levels in cells infected with either CTRC mutants p.A73T or p.G61R, in both AR42J cells and acini (Fig. 3A and B). When compared with WT CTRC, the recovery in tubulin acetylation was better achieved by cells infected with the p.A73T mutant (Fig. 3A and B).

3.5. SIRT2 inhibition improves amylase secretion in Cch-stimulated acinar cells and acini expressing ER stress-associated CTRC mutants

Subsequently, we evaluated the effects of SIRT2 inhibition on amylase secretion. In basal unstimulated conditions, AGK2 did not change neither amylase release (Fig. 3C and D) nor total amylase content (data not shown). While WT CTRC-control cells did not experience significant changes in Cch-stimulated amylase release due to incubation with AGK2 ($25.9 \pm 1.4\%$ and $27.7 \pm 1.5\%$ in AR42J cells and $29.7 \pm 1.8\%$ and $32.1 \pm 1.9\%$ in acini, respectively; Fig. 3C and D), CTRC p.A73T and p.G61R presented an improved Cch-stimulated amylase release in AGK2-treated cells ($17.9 \pm 1.2\%$ vs. $23.2 \pm 1.3\%$ and $13.9 \pm 0.9\%$ vs. $17.5 \pm 1.0\%$ in AR42J cells, and $22.2 \pm 1.4\%$ vs. $26.9 \pm 1.3\%$ and $17.4 \pm 1.4\%$ vs. $21.5 \pm 1.0\%$ in acini, respectively, representing an increase of 29.6% and 25.9% in AR42J cells, and 21.2% and 23.6% in acini, respectively; Fig. 3C and D).

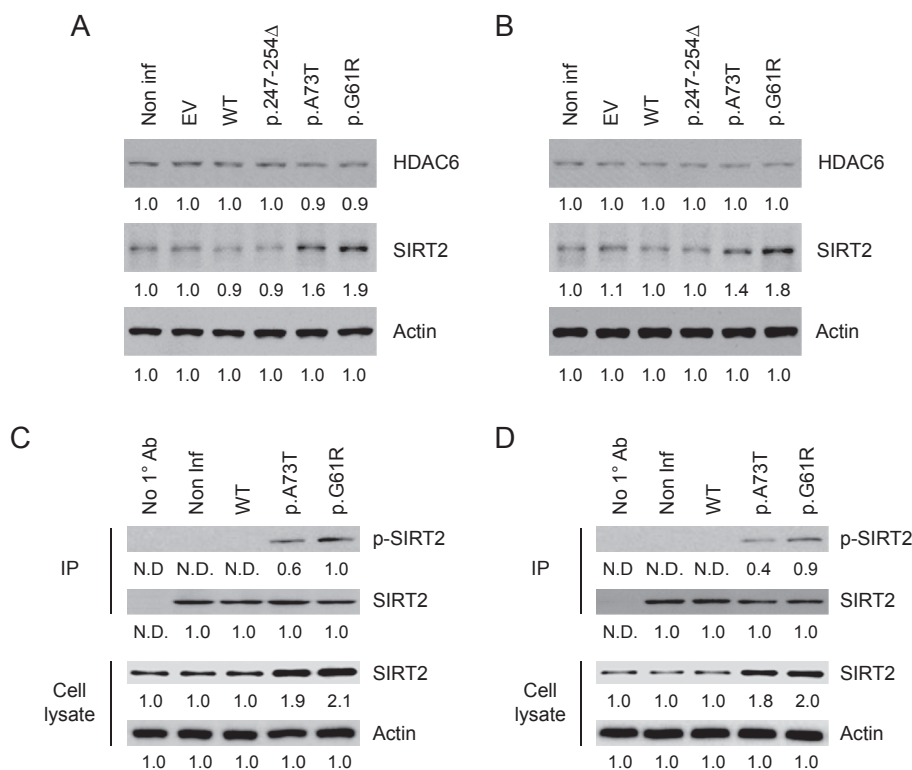


Fig. 2. SIRT2 expression and phosphorylation are elevated in acinar cells and acini expressing ER stress-associated CTRC mutants. (A–B) AR42J cells (A) and acini (B) were infected with EV, WT CTRC, p.247-254Δ CTRC, p.A73T CTRC or p.G61R CTRC, or were non infected (control). Levels of HDAC6, SIRT2, and actin (loading control) were analyzed in cell lysates of both infected and non infected cells. Representative immunoblots and densitometric analysis are shown. (C–D) AR42J cells (C) and acini (D) were infected with WT CTRC, p.A73T CTRC or p.G61R CTRC, or were non infected (control). Levels of SIRT2 and actin (loading control) were analyzed in cell lysates of both infected and non infected cells. In order to load equal amounts of SIRT2 for the immunoprecipitation (IP), samples of the CTRC mutants were diluted using levels in cell lysates as a reference. Levels of SIRT2 and phospho SIRT2 (p-SIRT2) were analyzed in the IP of both infected and non infected cells. Representative immunoblots and densitometric analysis are shown.

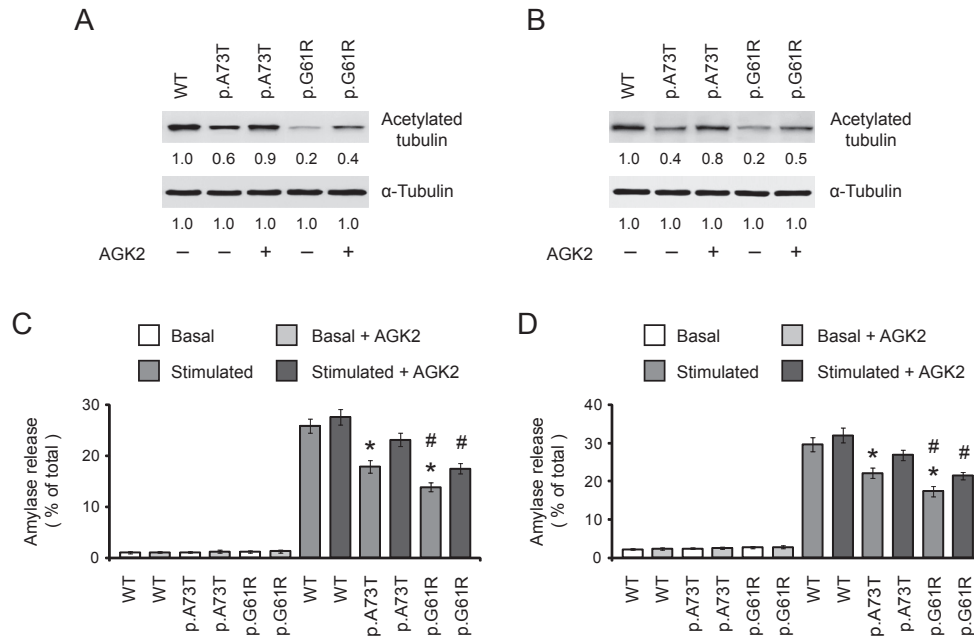


Fig. 3. Inhibition of SIRT2 greatly recovers tubulin acetylation levels as well as improves amylase secretion from Cch-stimulated acinar cells and acini expressing ER stress-associated CTIRC mutants. AR42J cells (A and C) and acini (B and D) were infected with WT CTIRC (control), p.A73T CTIRC or p.G61R CTIRC. (A–B) After 2 h treatment with the SIRT2 inhibitor AGK2 (15 μ M), levels of acetylated tubulin and α -tubulin (loading control) were analyzed in cell lysates of infected cells. Representative immunoblots and densitometric analysis are shown. (C–D). After 2 h incubation with AGK2 (15 μ M in KRH) or KRH alone, cells were stimulated with 80 μ M Cch for 1 h or further incubated with KRH, in the absence or presence of 15 μ M AGK2, as indicated. Amylase secreted into the media was determined and expressed as a percentage of the total cellular amylase. * $p < 0.05$ and # $p < 0.05$ compared to Cch-stimulated WT and p.A73T infected cells, respectively.

3.6. Secretion of ER stress-associated CTIRC mutants is not rescued by SIRT2 inhibition

We then examined the secretion of CTIRC under SIRT2 inhibition. In basal unstimulated conditions with or without AGK2 treatment, CTIRC was not detected in the supernatants of neither AR42J cells nor acini infected with either p.A73T or p.G61R (Fig. 4A and B). When compared to WT CTIRC, mutant p.A73T showed significant reduced levels of CTIRC in supernatants of both Cch-stimulated AR42J cells and acini, whereas no CTIRC was detected in the supernatants of both Cch-stimulated AR42J cells and acini infected

with p.G61R (Fig. 4A and B), being these results in line with a previous report [8]. Importantly, these Cch-stimulated secretions were not modified by AGK2 treatment (Fig. 4A and B).

4. Discussion

Microtubules are large filamentous structures assembled from dimers of α - and β -tubulin that can be subjected to a broad range of post-translational modifications such as acetylation, which is generally found in low turnover-stable microtubules. While lysine 40 (K40) acetylation is catalyzed by acetyl transferases α TAT/Mec-

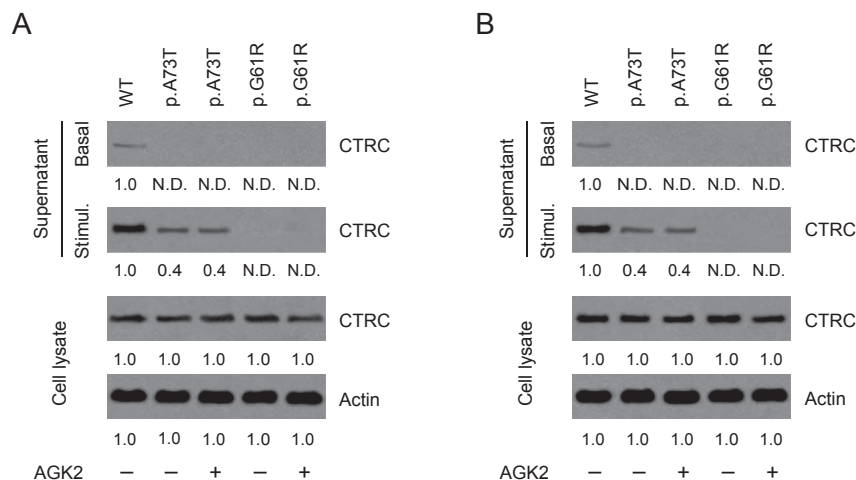


Fig. 4. Secretion of ER stress-associated CTIRC mutants is not rescued by SIRT2 inhibition. AR42J cells (A) and acini (B) were infected with WT CTIRC (control), p.A73T CTIRC or p.G61R CTIRC. After 2 h incubation with AGK2 (15 μ M in KRH) or KRH alone (basal conditions), cells were stimulated with 80 μ M Cch for 1 h in the absence or presence of 15 μ M AGK2, as indicated. CTIRC levels were analyzed in the supernatants of both unstimulated (basal) and stimulated conditions, as well as in cell lysates for which actin was used as loading control. Representative immunoblots and densitometric analysis are shown.

17, deacetylation is performed by HDAC6 and SIRT2 [19]. Unlike HDACs, sirtuin activity is intimately tied to the metabolic state of the cell [20].

All proteins that transit the secretory pathway in eukaryotic cells first enter the ER, where they fold and assemble into multi-subunit complexes. The efficiency of this process depends on appropriate environmental, genetic, and metabolic conditions. The high concentration of partially folded and unfolded proteins predisposes protein-folding intermediates to aggregate and represents a threat to cell viability. Polypeptide-binding proteins, such as BiP, act to slow protein-folding reactions and prevent aberrant interactions and aggregation. Persistent protein misfolding and oxidative stress initiate apoptotic cascades and are now known to play predominant roles in the pathogenesis of multiple human diseases including diabetes, atherosclerosis, and neurodegenerative diseases [21].

Unfolded protein accumulation in the ER may elicit Ca^{2+} leak into the cytosol that increases reactive oxygen species (ROS) production in mitochondria. Furthermore, both protein folding and refolding in the ER lumen are highly energy-dependent processes. Thus, ATP depletion as a consequence of protein misfolding could stimulate mitochondrial oxidative phosphorylation to increase ATP production, and consequently increase ROS production [21].

Oxidative stress, such as hydrogen peroxide (H_2O_2) treatment, increases SIRT2 expression in several cell types, including human embryonic kidney HEK293T cells, murine 3T3-L1 adipocytes, and rat pheochromocytoma PC12 cells [22,23]. Furthermore, over-expression of SIRT2 in mouse NIH/3T3 fibroblasts enhances both caspase-3 mediated and caspase-3 independent cell death when cells are exposed to severe stress [22]. Consistently, either SIRT2 silencing or pharmacological inhibition of SIRT2 activity decreases H_2O_2 -induced apoptosis in PC12 cells, partially by inhibiting caspase-3 activation [23]. This indicates that our result showing an increase in the expression and phosphorylation levels of SIRT2 (Fig. 2) is in agreement with the previously found increase in caspase-3/7 activity and apoptosis in AR42J cells expressing p.A73T CTRC [10].

Treatment of ameloblast-derived LS8 cells with high doses of fluoride induces ER-stress and the expression of unfolded protein response transcription factors in a dose-dependent manner, as well as caspase-mediated apoptosis [24,25]. Remarkably, fluoride treatment increases SIRT1 expression and phosphorylation, resulting in an elevated deacetylase activity [25], as well as decreases extracellular secretion of the proteinases matrix metalloproteinase-20 and kallikrein-4 [24]. This seems to correlate with our finding on SIRT-2-mediated inhibition of amylase secretion.

In secretory cells, microtubule-based motor enzymes support the transport of secretory vesicles to the cell surface for subsequent release [14]. Although little is known about the functions of K40 acetylation, some studies suggest a regulation of kinesin motors [19]. In both primary hippocampal neurons and CAD cells, acetylated microtubules have been shown to serve as 'high occupancy vesicle' lanes for kinesin-mediated anterograde transport of JIP1-containing vesicles to the tips of neuritis [26]. Studies on the dynamic properties of brain-derived neurotrophic factor (BDNF)-containing vesicles in striatal cells indicate that microtubule acetylation stimulates not only anterograde but also retrograde transport, through the recruitment of both anterograde (kinesin) and retrograde (dynein) motors [25]. Likewise, HDAC inhibitors increase vesicular transport and the subsequent release of BDNF in striatal cells [27].

From our present work, we conclude that CTRC variants associated to ER stress increase SIRT2 expression and activity. As a consequence, microtubules become less stable and

secretagogue-stimulated pancreatic zymogen secretion is inhibited. Of note, the extent of this inhibition correlates with the degree of ER stress exhibited by the particular CTRC variant.

Conflict of interest

No conflicts of interest to declare.

Acknowledgments

This work was supported by research grants given to Dr Cosen-Binker by KB Certification International. We also thankfully acknowledge the support of Prof. Miklos Sahin-Toth and David Levine (Department of Cellular and Molecular Biology - Boston University).

Transparency document

Transparency document related to this article can be found online at <http://dx.doi.org/10.1016/j.bbrc.2015.05.064>.

References

- [1] M. Sachs, Study of the pancreas and its inflammatory diseases from the 16th–19th century, *Zentralbl. Chir.* 118 (1993) 702–711.
- [2] H.Y. Gaisano, F.S. Gorelick, New insights into the mechanisms of pancreatitis, *Gastroenterology* 136 (2009) 2040–2044.
- [3] S. Willemer, R. Bialek, G. Adler, Localization of lysosomal and digestive enzymes in cytoplasmic vacuoles in caerulein-pancreatitis, *Histochemistry* 94 (1990) 161–170.
- [4] L.I. Cosen-Binker, H.Y. Gaisano, Recent insights into the cellular mechanisms of acute pancreatitis, *Can. J. Gastroenterol.* 21 (2007) 19–24.
- [5] M.S. Cappell, Acute pancreatitis: etiology, clinical presentation, diagnosis, and therapy, *Med. Clin. North. Am.* 92 (2008) 889–923.
- [6] D.C. Whitcomb, M.E. Lowe, Hereditary, familial and genetic disorders of the pancreas and pancreatic disorders in childhood, in: M. Feldman, L.S. Friedman, M.H. Sleisenger (Eds.), *Sleisenger and Fordtran's Gastrointestinal and Liver Disease*, 9 ed, WB Saunders Company, Philadelphia, PA, 2010, pp. 931–957.
- [7] J. Zhou, M. Sahin-Toth, Chymotrypsin C mutations in chronic pancreatitis, *J. Gastroenterol. Hepatol.* 26 (2011) 1238–1246.
- [8] S. Beer, J. Zhou, A. Szabo, et al., Comprehensive functional analysis of chymotrypsin C (CTRC) variants reveals distinct loss-of-function mechanisms associated with pancreatitis risk, *Gut* 62 (2013) 1616–1624.
- [9] J. Rosendahl, H. Witt, R. Szmola, et al., Chymotrypsin C (CTRC) variants that diminish activity or secretion are associated with chronic pancreatitis, *Nat. Genet.* 40 (2008) 78–82.
- [10] R. Szmola, M. Sahin-Toth, Pancreatitis-associated chymotrypsinogen C (CTRC) mutant elicits endoplasmic reticulum stress in pancreatic acinar cells, *Gut* 59 (2010) 335–372.
- [11] J. Kraemer, F. Schmitz, D. Drenckhahn, Cytoplasmic dynein and dynactin as likely candidates for microtubule-dependent apical targeting of pancreatic zymogen granules, *Eur. J. Cell. Biol.* 78 (1999) 265–277.
- [12] S. Muallem, K. Kwiatkowska, X. Xu, H.L. Yin, Actin filament disassembly is a sufficient final trigger for exocytosis in nonexcitable cells, *J. Cell. Biol.* 128 (1995) 589–598.
- [13] J.A. Williams, M. Lee, Microtubules and pancreatic amylase release by mouse pancreas in vitro, *J. Cell. Biol.* 71 (1976) 795–806.
- [14] K.J. Marlowe, P. Farshori, R.R. Torgerson, et al., Changes in kinesin distribution and phosphorylation occur during regulated secretion in pancreatic acinar cells, *Eur. J. Cell. Biol.* 75 (1998) 140–152.
- [15] T. Ueda, Y. Takeyama, M. Adachi, et al., Effect of the microtubule-disrupting drug colchicine on rat cerulein-induced pancreatitis in comparison with the microtubule stabilizer taxol, *Pancreas* 11 (1995) 294–302.
- [16] C.D. Logsdon, J. Moessner, J.A. Williams, I.D. Goldfine, Glucocorticoids increase amylase mRNA levels, secretory organelles, and secretion in pancreatic acinar AR42J cells, *J. Cell. Biol.* 100 (1985) 1200–1208.
- [17] H.Y. Gaisano, U.G. Klueppelberg, D. Pinon, et al., A novel tool for the study of CCK-stimulated pancreatic enzyme secretion, *J. Clin. Invest.* 83 (1989) 321–325.
- [18] H.Y. Gaisano, M.P. Lutz, G. Lynch, et al., Supramaximal cholecystokinin displaces Munc18c from the pancreatic acinar basal surface, redirecting apical exocytosis to the basal membrane, *J. Clin. Invest.* 108 (2001) 1597–1611.
- [19] C. Janke, The tubulin code: molecular components, readout mechanisms, and functions, *J. Cell. Biol.* 206 (2014) 461–472.
- [20] M.C. Haigis, D.A. Sinclair, Mammalian sirtuins: biological insights and disease relevance, *Annu. Rev. Pathol.* 5 (2010) 253–295.

- [21] J.D. Malhotra, R.J. Kaufman, Endoplasmic reticulum stress and oxidative stress: a vicious cycle or adouble-edged sword? *Antioxid. Redox Signal* 9 (2007) 2277–2293.
- [22] F. Wang, M. Nguyen, F.X. Qin, Q. Tong, SIRT2 deacetylates FOXO3a in response to oxidative stress and caloric restriction, *Aging Cell*. 6 (2007) 505–514.
- [23] H. Nie, Y. Hong, X. Lu, et al., SIRT2 mediates oxidative stress-induced apoptosis of differentiated PC12 cells, *Neuroreport* 25 (2014) 838–842.
- [24] W. Wei, Y. Gao, C. Wang, et al., Excessive fluoride induces endoplasmic reticulum stress and interferes enamel proteinases secretion, *Environ. Toxicol.* 28 (2013) 332–341.
- [25] M. Suzuki, J.D. Bartlett, Sirtuin1 and autophagy protect cells from fluoride-induced cell stress, *Biochim. Biophys. Acta* 1842 (2014) 245–255.
- [26] N.A. Reed, D. Cai, T.L. Blasius, et al., Microtubule acetylation promotes kinesin-1 binding and transport, *Curr. Biol.* 16 (2006) 2166–2172.
- [27] J.P. Dompierre, J.D. Godin, B.C. Charrin, et al., Histone deacetylase 6 inhibition compensates for the transport deficit in Huntington's disease by increasing tubulin acetylation, *J. Neurosci.* 27 (2007) 3571–3583.